Extreme-Mass-Ratio-Black-Hole-Binary Evolutions with Numerical Relativity

Carlos O. Lousto and Yosef Zlochower

Center for Computational Relativity and Gravitation,
School of Mathematical Sciences, Rochester Institute of Technology,
85 Lomb Memorial Drive, Rochester, New York 14623
(Dated: September 1, 2010)

We perform full numerical simulations of black-hole binaries with mass ratios 100:1. Our technique for evolving such extreme mass ratios is based on the moving puncture approach with a new gauge condition and an optimal choice of the mesh refinement (plus large computational resources). We achieve a convergent set of results for simulations starting with a small nonspinning black hole near the ISCO that then performs over two orbits before plunging into the one hundred times more massive black hole. We compute the gravitational energy and momenta radiated as well as the final remnant parameters and compare those quantities with the corresponding perturbative estimates. The results show a close agreement. We briefly discuss the relevance of this simulations for advanced LIGO and LISA observers, and self-force computations.

PACS numbers: 04.25.dg, 04.30.Db, 04.25.Nx, 04.70.Bw

Introduction: The orbital evolution and computation of gravitational radiation from black hole binaries (BHB) in the small-mass-ratio limit remains one of the most challenging problems in General Relativity. This was recognized early on by Regge and Wheeler over fifty years ago [1]. Zerilli then completed the formulation of the first order perturbations around a Schwarzschild black hole in 1970 [2]. Three years later, Teukolsky [3] provided a new formalism to study perturbations around Kerr black holes. In order to take into account the decay of the small black hole orbit due to the emission of gravitational radiation, second order effects have to be included in those computations. This problem turned to be very challenging, and only since 1996 [4, 5] has there been a consistent formalism for the "self-force" corrections to the background geodesic motion of a small BH orbiting around a larger one. The explicit implementation of such formalism into a computational scheme remains challenging, although recent progress along this line is encouraging [6].

The dramatic breakthroughs in the numerical techniques to evolve BHBs [7–9] transformed the field of Numerical Relativity (NR) and we are now in position to evolve binary systems in an intermediate mass ratio regime. Two years ago the merger of spinning [10] binaries bearing a mass ratio $q = m_1/m_2 = 1/8$ and nonspinning binaries[11] with $q = 1/10$ were published. More recently, detailed long term evolutions of BHBs with $q = 1/10$ and $q = 1/15$ were studied and validated against perturbation theory [12, 13]. In this letter we present the first full numerical results of the merger of extreme mass ratio BHBs. As a case study, we evolve a nonspinning BHB with mass ratio $q = 1/100$ for over two orbits prior to merger, and resolve the entire waveform for three grid resolutions, proving numerical convergence of the results. The success of our approach is based on an enhancement of the moving puncture numerical techniques by adapting the gauge and grid structure for the small mass ratio limit, and the use of massive computational resources.

TABLE I: Initial data parameters. The punctures are located on the x-axis at positions x_1 and x_2, with puncture mass parameters (not horizons masses) m_1 and m_2, and momentum $\pm\vec{p}$. The punctures have zero spin.

x_1	4.952562636	p_x	-0.00001026521884
x_2	-0.04743736368	p_y	0.00672262416584
m_1	0.00868947461701704882	$M_{\rm ADM}$	1.00000000005
m_2	0.98961921419277897684	q	0.01000004

The techniques described in this letter can used in the spinning BHB case and for even smaller mass ratio inspirals. This has important consequences for astrophysics and gravitational wave observatories as advanced LIGO and LISA. Supermassive black hole collision at cosmological scales are most likely to occur in the mass ratio range 1:10 - 1:100 [14] and be observed by LISA [15]. While collision of intermediate mass BHs and solar mass BHs will lie in the Advanced LIGO sensitivity band [16].

Fully Nonlinear Numerical Simulations: In Table I we give the initial data parameters for our $q = 1/100$ BHB simulations. We evolved this BHB data-set using the LazEv [17] implementation of the moving puncture approach [8, 9]. Our code used the Cactus toolkit [18] and the Carpet [19] mesh refinement driver to provide a 'moving boxes' style mesh refinement.

We obtain accurate, convergent waveforms and horizon parameters by evolving this system in conjunction with a modified 1+log lapse and a modified Gamma-driver

shift condition [8, 20], and an initial lapse $\alpha(t=0) = 2/(1+\psi_{BL}^4)$. The lapse and shift are evolved with

$$(\partial_t - \beta^i\partial_i)\alpha = -2\alpha K, \quad (1)$$

$$\partial_t\beta^a = (3/4)\tilde{\Gamma}^a - \eta(x^a,t)\beta^a, \quad (2)$$

where different functional dependences for $\eta(x^a,t)$ have been proposed in [17, 21–25]. Here we use a modification of the form proposed in [22],

$$\eta(x^a,t) = R_0\frac{\sqrt{\partial_i W\partial_j W\tilde{\gamma}^{ij}}}{(1-W^a)^b}, \quad (3)$$

where we chose $R_0 = 1.31$. The above gauge condition is inspired by, but differs from Ref. [22] between the BHs and in the outer zones when $a \neq 1$ and $b \neq 2$.Once the conformal factor settles down to its asymptotic $\psi = C/\sqrt{r} + O(1)$ form near the puncture, η will have the form $\eta = (R_0/C^2)(1 + b(r/C^2)^a)$ near the puncture and $\eta = R_0 r^{b-2}M/(aM)^b$ as $r \to \infty$. In practice we used $a = 2$ and $b = 2$, which reduces η by a factor of 4 at infinity when compared to the original version of this gauge proposed by [22]. We note that if we set $b = 1$ then η will have a $1/r$ falloff at $r = \infty$ as suggested by [24].

According to Chandrasekhar [26, p160] the even/odd parity effective potentials of a Schwarzschild black hole can be written as

$$V_\ell^\pm = \pm 6M\frac{df}{dr^*} + (6M)^2 f^2 + 4\lambda(\lambda+1)\, f, \quad (4)$$

where

$$f = \frac{(r-2M)}{2r^2(\lambda r + 3M)}, \quad \lambda = \frac{1}{2}(\ell+2)(\ell-1). \quad (5)$$

Note that both potentials are very close to each other, hence we consider for guiding our grid structure (in isotropic coordinates R)

$$\frac{d(V_\ell^+ + V_\ell^-)}{dR}, \quad r = R\left(1+\frac{M}{2R}\right)^2. \quad (6)$$

which for $\ell = 2$ and $M = 1$ take the explicit form

$$\left.\frac{d(V^+ + V^-)}{dR}\right|_{\ell=2,M=1} = \quad (7)$$
$$-384\,\frac{R\,(2\,R-1)\left(16\,R^4 - 4\,R^3 - 60\,R^2 - R + 1\right)}{(2\,R+1)^9\,(4\,R^2+10\,R+1)^3} \times$$
$$\left(64R^6 + 288R^5 + 480R^4 + 256R^3 + 120R^2 + 18R + 1\right).$$

This function has zeros at $R/M = 0.0, 0.1207998431$ inside the horizon and $R/M = 0.5, 2.069539112$, where we ideally would like to locate the boundaries of the refinement levels since there is the least change. In particular, since we do not want to over-resolve the interior, this suggests that the crucial region we should numerically resolve lies between the horizon and nearly for times its radius in quasi-isotropic coordinates.

In Ref. [13] we provide an alternative method of extrapolation of waveforms based on a perturbative propagation of the asymptotic form of ψ_4 at large distances from the sources leading to the following simple expression

$$\lim_{r\to\infty}[r\,\psi_4^{\ell m}(r,t)] = \quad (8)$$
$$\left[r\,\psi_4^{\ell m}(r,t) - \lambda\int_0^t dt\,\psi_4^{\ell m}(r,t)\right]_{r=r_{\rm Obs}} + O(r_{\rm Obs}^{-2}),$$

where $r_{\rm Obs}$ is the approximate areal radius of the sphere This formula is applicable for $r_{\rm Obs} \gtrsim 100M$.

Note that it is also important to remove the low frequency components in ψ_4 (since it is inside an integral).

Results and Analysis: Our simulation used 15 levels of refinement (around the smaller components), with central resolutions as high as $M/7077$, and 9 levels of refinement around the larger component. The outer boundaries were located at $400M$ and the resolution in the boundary zone was $h = 2.3148M$ for our finest resolution run. The BHB performs ~ 2 orbits prior to merger (as seen by the formation of a common apparent horizon (CAH)), which occurs roughly $160M$ after the start of the simulation.

Table II shows the results of evolution. We note that the we find that the smaller BH mass is conserved to within 0.23% during the inspiral and plunge phases, while the mass of the larger BH is conserved to within 0.003%. In Fig. 1 we show the xy projection of the orbital trajectories for the two highest resolution runs. From the figure we can see that the initial jump in the orbit pushes the binary slightly outside the ISCO leading to an additional orbit. In Fig. 2 we show the orbital radius as a function of time and resolution. Note that the orbital radius superconverges at low resolution and converges quadratically at high resolution (indicating that time prolongation effects are important). In Fig. 3 we show the imaginary part of the $(\ell = 2, m = 2)$ mode of ψ_4 (the real part shows considerable noise to due AMR boundary reflections of the initial burst), as well the eighth-order convergence of the phase of this mode.

The apparent superconvergence in the trajectories and waveforms when considering the three coarsest resolutions is indicative that the lowest resolution is just entering the convergence regime. That is, this resolution cannot be far from the convergence regime because all four resolutions lie in a monotonic convergence sequence. And importantly, the deviations between the next three resolution are very small compared to the deviation between the lowest two resolutions, indicating that these three resolutions are safely inside the convergence regime.

Finally, in Fig. 4 we show the remnant spins and total radiated mass as a function of mass ratio for $q = 1/10, 1/15, 1/100$ and the predictions based on our empirical formula [27]. Note that no fitting is involved in

TABLE II: Remnant horizon parameters and radiated energy-momentum. Here we provide $\delta M_H^* = M_{\rm ADM} - M_H$ and $\delta S_H^* = J_{ADM} - S_H$, which are small numbers obtained by taking the difference between two much larger numbers. The calculation of δS_H is relatively inaccurate because it requires an extrapolation to infinite resolution.

E_{rad}	0.000060 ± 0.000001	δM_H^*	0.00007 ± 0.00001
J_{rad}	0.00050 ± 0.00002	δS_H^*	0.0003 ± 0.0002
α	0.0333 ± 0.0002		

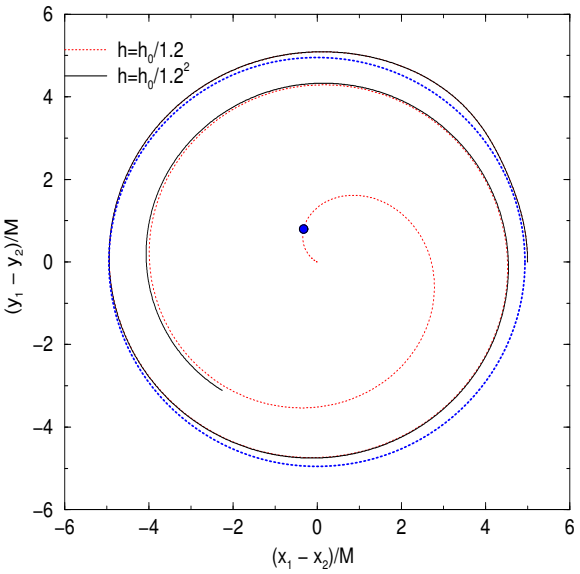

FIG. 1: An xy projection of the trajectories for the two highest resolutions of the $q = 1/100$ configuration. The dotted circle corresponds to the ISCO radius while the small filled in circle corresponds to the point on the trajectory where a common horizon is first detected. Note the initial "jump" in radius (see Fig. 2).

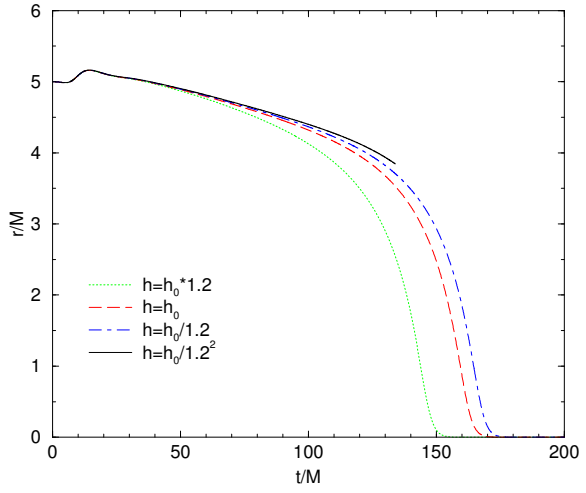

FIG. 2: The orbital radius as a function of time and resolution for the $q = 1/100$ configuration. Note the initial "jump" in the orbit due to the initial data.

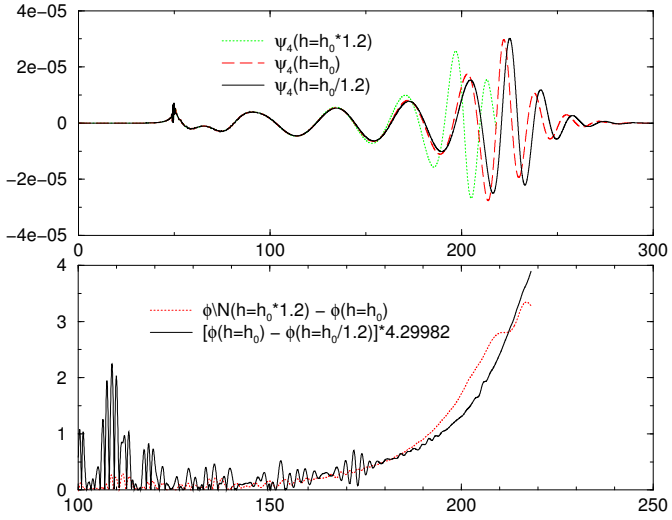

FIG. 3: The imaginary part of the $(\ell = 2, m = 2)$ mode of ψ_4 (which is less noisy than the real part) and the convergence of the phase ϕ of this mode. Note that the phase converges to eighth order at these resolutions.

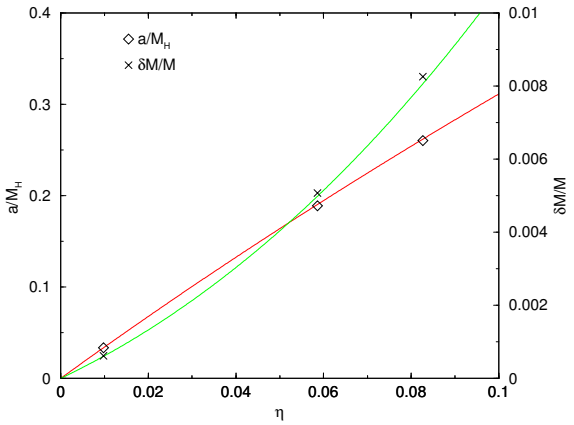

FIG. 4: The remnant spin a/M_H and the radiated mass from infinite separation $\delta M/M$, as a function of the symmetric mass ratio $\eta = q/(1+q)^2$, for $q = 1/10,\ 1/15,\ 1/100$, as well as the empirical formula prediction.

this figure.

The amount of energy and angular momentum radiated when the $(2,2)$ mode frequency is larger than $\omega_{2,2} > 0.167$ is given by $\delta E = 0.000047 \pm 0.000001$ and $\delta J = 0.00034 \pm 0.00001$, which agrees to within 4% with the particle limit predictions of $\delta E/M = 0.47\eta^2$ and $\delta J/M^2 = 3.44\eta^2$ [28].

Conclusions and Discussion: We have successfully evolved a 1:100 BBH system for the last couple of orbits before merger and down to the final Kerr hole remnant. We have achieved this within the moving punctures approach by adapting the gamma-driver shift condition with a variable damping term. Also crucial for evolu-

TABLE III: Remnant spin and total radiated mass (starting from infinite separation) as a function of mass ratio q as measured in our simulations and as predicted by our empirical formulae.

q	1/10	1/15	1/100
α (Comp)	0.2603	0.18875	0.0333
α (Pred)	0.2618	0.1903	0.03358
δM (Comp)	0.00826	0.00507	0.000618
δM (Pred)	0.00806	0.00498	0.000604

tions is an optimal choice of the mesh refinement structure around the small black hole. We used the Regge-Wheeler-Zerilli potentials to guide the setting up of the initial grids. This helps optimizing the large resources required to evolve small q binaries. The numerical convergence of the waveforms displayed here and the successful comparisons with perturbative results [12, 13] show this approach is validated in the intermediate mass ratio region and can be applied to even smaller q's (and larger initial separations into the post-Newtonian regime).

The feasibility of simulating extreme mass ratios by purely full numerical methods as demonstrated in this work allow us to look more optimistically at the task of generating a bank of templates for both Advanced LIGO and LISA gravitational wave detectors [29]. Methods like those described in [12, 13], that combine NR and perturbative techniques can be used to speed up the generation of those templates. And finally we now have a direct way of validating self-force computations [6].

The techniques presented here should straightforwardly apply to even smaller mass ratios q and to initially spinning black holes. Fine tuning of the quasicircular orbital parameters plays an important role in preparing these runs given the very low level of gravitational radiation they generate. So far we see that the method [30] developed for equal mass BBHs to lower e seems still to work, but it requires extra runs for experimentation. Hence it would be important to evolve initial data with lower spurious radiation content and some true inspiral wave information [31].

We gratefully acknowledge NSF for financial support from grants PHY-0722315, PHY-0653303, PHY-0714388, PHY-0722703, DMS-0820923, PHY-0969855 and PHY-0929114; and NASA for financial support from grants NASA 07-ATFP07-0158 and HST-AR-11763. Computational resources were provided by Ranger cluster at TACC (Teragrid allocation TG-PHY060027N) and by NewHorizons at RIT.

[1] T. Regge and J. Wheeler, Phys. Rev. **108**, 1063 (1957).
[2] F. J. Zerilli, Phys. Rev. D **2**, 2141 (1970).
[3] S. A. Teukolsky, Astrophys. J. **185**, 635 (1973).
[4] Y. Mino, M. Sasaki, and T. Tanaka, Phys. Rev. **D55**, 3457 (1997), gr-qc/9606018.
[5] T. C. Quinn and R. M. Wald, Phys. Rev. **D56**, 3381 (1997), gr-qc/9610053.
[6] L. Barack and N. Sago, Phys. Rev. **D81**, 084021 (2010), 1002.2386.
[7] F. Pretorius, Phys. Rev. Lett. **95**, 121101 (2005), gr-qc/0507014.
[8] M. Campanelli, C. O. Lousto, P. Marronetti, and Y. Zlochower, Phys. Rev. Lett. **96**, 111101 (2006), gr-qc/0511048.
[9] J. G. Baker, J. Centrella, D.-I. Choi, M. Koppitz, and J. van Meter, Phys. Rev. Lett. **96**, 111102 (2006), gr-qc/0511103.
[10] C. O. Lousto and Y. Zlochower, Phys. Rev. D **79**, 064018 (2009), 0805.0159.
[11] J. A. Gonzalez, U. Sperhake, and B. Brugmann, Phys. Rev. **D79**, 124006 (2009), 0811.3952.
[12] C. O. Lousto, H. Nakano, Y. Zlochower, and M. Campanelli, Phys. Rev. Lett. **104**, 211101 (2010), 1001.2316.
[13] C. O. Lousto, H. Nakano, Y. Zlochower, and M. Campanelli (2010), 1008.4360.
[14] M. Volonteri and P. Madau, Astrophys. J. **687**, L57 (2008), 0809.4007.
[15] C. M. Will, Astrophys. J. **611**, 1080 (2004), astro-ph/0403644.
[16] I. Mandel, D. A. Brown, J. R. Gair, and M. C. Miller, Astrophys. J. **681**, 1431 (2008), 0705.0285.
[17] Y. Zlochower, J. G. Baker, M. Campanelli, and C. O. Lousto, Phys. Rev. D **72**, 024021 (2005), gr-qc/0505055.
[18] *Cactus:* `http://www.cactuscode.org`.
[19] E. Schnetter, S. H. Hawley, and I. Hawke, Class. Quantum Grav. **21**, 1465 (2004), gr-qc/0310042.
[20] M. Alcubierre, B. Brügmann, P. Diener, M. Koppitz, D. Pollney, E. Seidel, and R. Takahashi, Phys. Rev. D **67**, 084023 (2003), gr-qc/0206072.
[21] M. Alcubierre, B. Brügmann, P. Diener, F. Herrmann, D. Pollney, E. Seidel, and R. Takahashi, submitted to Phys. Rev. D (2004), gr-qc/0411137.
[22] D. Mueller and B. Bruegmann, Class. Quant. Grav. **27**, 114008 (2010), 0912.3125.
[23] D. Mueller, J. Grigsby, and B. Bruegmann (2010), 1003.4681.
[24] E. Schnetter, Class. Quant. Grav. **27**, 167001 (2010), 1003.0859.
[25] D. Alic, L. Rezzolla, I. Hinder, and P. Mosta (2010), 1008.2212.
[26] S. Chandrasekhar, *The mathematical theory of black holes* (1983).
[27] C. O. Lousto, M. Campanelli, Y. Zlochower, and H. Nakano, Class. Quant. Grav. **27**, 114006 (2010), 0904.3541.
[28] S. Bernuzzi and A. Nagar, Phys. Rev. **D81**, 084056 (2010), 1003.0597.
[29] I. Mandel and J. R. Gair, Class. Quant. Grav. **26**, 094036 (2009), 0811.0138.
[30] H. P. Pfeiffer et al., Class. Quant. Grav. **24**, S59 (2007), gr-qc/0702106.
[31] B. J. Kelly, W. Tichy, Y. Zlochower, M. Campanelli, and B. F. Whiting, Class. Quant. Grav. **27**, 114005 (2010), 0912.5311.